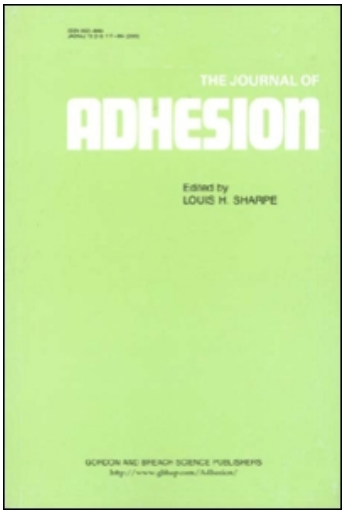

The Journal of Adhesion
Publication details, including instructions for authors and subscription information:
http://www.informaworld.com/smpp/title~content=t713453635

Indentation-debonding of an Adhered Surface Layer

P. A. Engel; D. D. Roshon

To cite this Article Engel, P. A. and Roshon, D. D.(1979) 'Indentation-debonding of an Adhered Surface Layer', The Journal of Adhesion, 10: 3, 237 — 253
To link to this Article: DOI: 10.1080/00218467908544627
URL: http://dx.doi.org/10.1080/00218467908544627

J. Adhesion, 1979, Vol. 10, pp. 237–253
0021–8464/79/1003–0237 $04.50/0

Printed in Great Britain

Indentation-debonding of an Adhered Surface Layer†

P. A. ENGEL and D. D. ROSHON

IBM Corporation, System Products Division, Endicott, New York 13760, U.S.A.

(*Received December 12, 1978; in final form June 11, 1979*)

In many technological applications (e.g. circuitboards), relatively thin, soft polymer layers are bonded to a harder (metal) surface. A new mechanical test for the adhesive bond strength between these layers using sharp, needle-like indenters, has been developed. This test and its experimental-analytical features are described in this paper. In the central indented region of the bonded polymer, compressive deformations of the top layer and subsurface take place. At the rim of the central indented area, however, a tensile stress is induced in the interfacial bond between the top layer and the substrate. Debonding occurs when this stress exceeds the bond strength. A debonded polymer surface layer displays Newton's rings because it diffracts light. Observations indicate that the debonded segment of the surface layer behaves as an elastic plate between the rim of indentation and the unfailed bonded region. The "peeling moment" capacity of adhesive at the bonded edge limits the bond resistance. Considering the latter as a constant parameter (a characteristic of the bond) a relation predicting the debonded radius in terms of the indenting force is derived.

INTRODUCTION

Many industries employ thin, adhered layers in laminated constructions. In these assemblies, the several layers of various types of rigidity and thickness must perform as a structural unit. The present investigation originated from the authors' search for a convenient, reliable test procedure, whereby the adhesion of an epoxy‡ layer (of approximately 25 μm thickness) bonded onto copper substrates could be verified. The total structure was multilaminar circuitboard, with repeated successive pattern of epoxy and copper layers.

† Presented at the VIII U.S. National Congress of Theoretical and Applied Mechanics, Los Angeles, California, June, 1978.

‡ The material of the top polymer (epoxy) layer was a modified high-functionality epoxy resin.

This structure is sensitive to local (contact) stresses arising from scratching and handling. In the new test[1] proposed and successfully implemented by the authors, a sharp, needle-like indenter is pressed with moderate force (less than 1 kgf) against a small sample of the layered medium, and the indentation is simultaneously viewed under a microscope to detect any debonding that occurs.

This paper pursues three main objectives: (1) a description of the indentation debonding phenomenon; (2) an introduction of the experimental equipment and the principal parameters emerging from the experiments; and (3) a derivation of an engineering analysis method to estimate a relationship between the force, debonded area and adhesion.

The model found valid in this study considers the plastic deformations arising in metallic sublayers. Force-displacement relations must be established empirically because the multilaminar construction makes analysis intractable. Debonding, in general, may involve failures through both the material of the top layer and through the sublayer; in this study, emphasis was placed on purely interfacial debonding. In fact, to facilitate observation of the phenomenon, and to reveal basic relationships, the bond in test specimens was often intentionally degraded† during the process of preparation to force interfacial separation between polymer top layer and metal substrate.

EXPERIMENTAL

Experimental work was performed on multilaminar structures such as the structure shown in cross section in Figure 1. Indenter tips were applied initially through a Knoop hardness tester because the latter allows a slow and gradual application of the indenting force. Figure 2 shows the profiles of these (mostly axially symmetric) indenter tips which were made of hard steel. They were checked for any significant deformation (blunting) after each indentation-debonding test, with a consistently negative result. When the indenter was applied more rapidly, no basic difference was observed indicating that inertia effects can be usually neglected, and deformation is not rate sensitive.

Upon pressing the indenter against the layered surface, the debonding proceeded along roughly concentric circular areas around the indentation. The debonded thin film enclosed a prism of vacuum confined on the other side by the metal (copper) substrate. Interference patterns (Newton's rings) were visible in the debonded area, Figure 3.

† A degraded adhesive bond was obtained by polishing the metal surface with wet-dry paper; a dip into 10% HCl acid solution, rinsing, and drying followed. The epoxy top layer was subsequently applied to the metal surface.

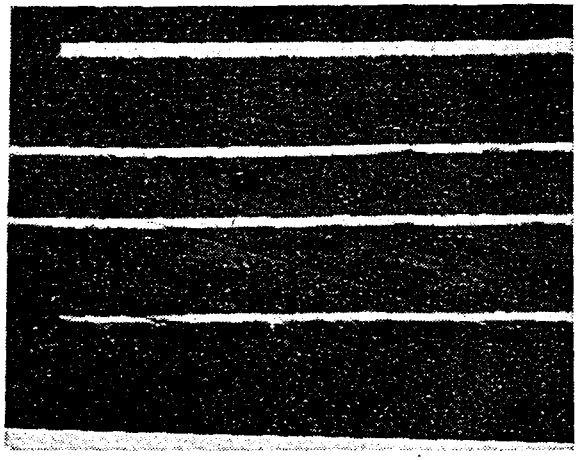

FIGURE 1 Cross-section of circuitboard showing several layers of copper and epoxy plastic layers (50×).

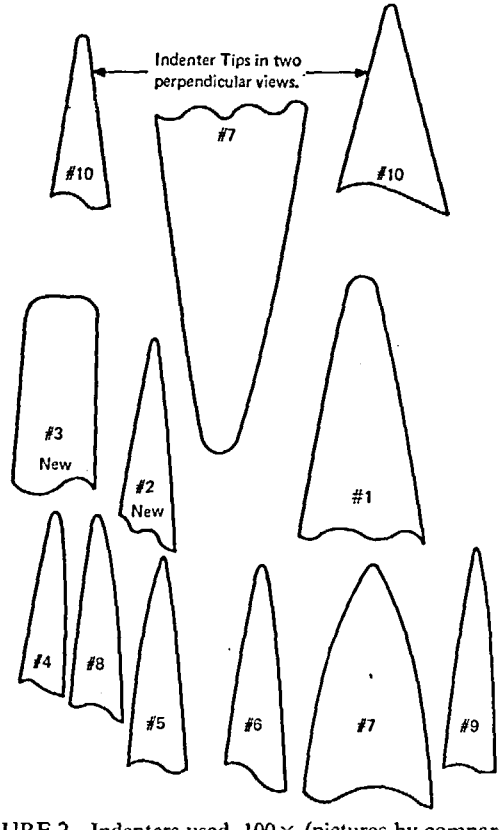

FIGURE 2 Indenters used. 100× (pictures by comparator).

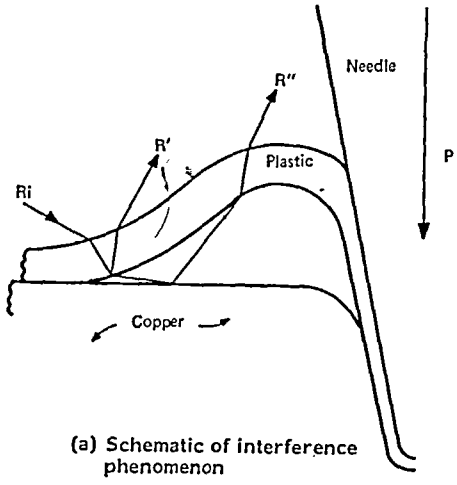

(a) Schematic of interference phenomenon

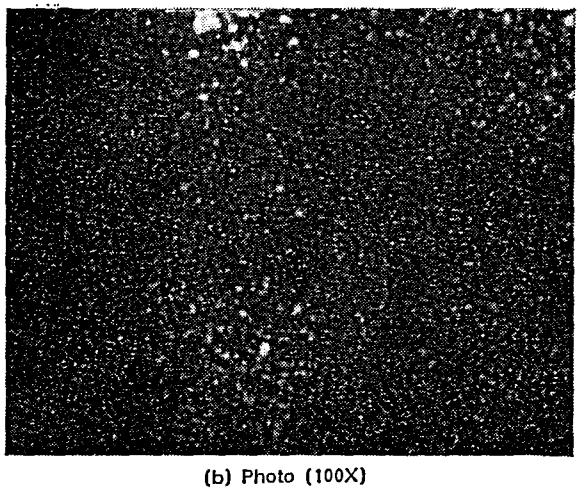

(b) Photo (100X)

FIGURE 3 Newton's rings resulting from typical indentation debonding of epoxy layer previously adhered to a copper substrate.

The rings greatly facilitate the observation process. As the indenting force was increased, the indentation area also increased. The debonded area widened around it, with the addition of more Newton's rings.

The indentation-debonding phenomenon is explained as follows (Figure 4). When a sharp indenter is pressed against the surface of the laminate, the

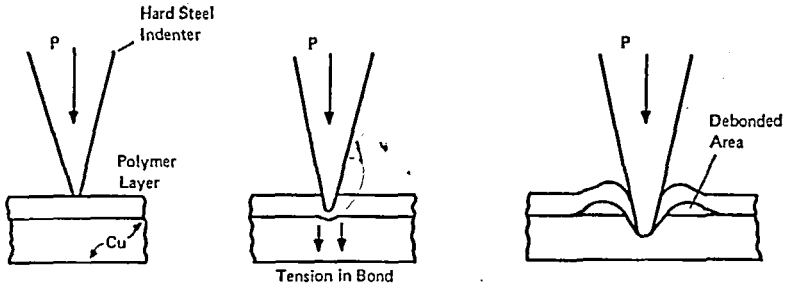

FIGURE 4 Sequence of events leading to debonding of polymer layer from a metal substrate.

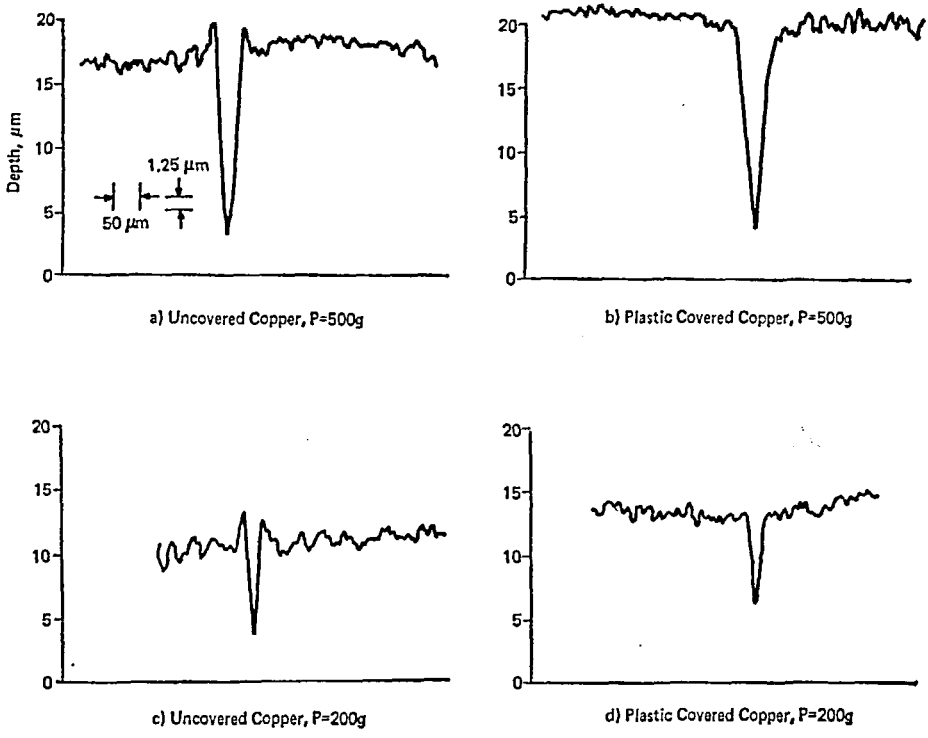

FIGURE 5 Talysurf profiles of indentations of copper substrates with #5 indenter ($\tan \theta_o = -2.2$).

topmost metal (copper) layer is plastically deformed. As the polymer is pushed into the cavity, large normal stresses arise on the interface of the metal and polymer material. Under the contact zone these stresses are compressive, but outside the contact circle tension develops. When the tensile stresses reach the critical magnitude, debonding occurs. The debonding spreads until its perimeter is large enough to support the tensile stress. The indenter tip may actually punch a small hole in the top layer. This does not relieve the tensile stress on the interface since a great deal of friction exists between the indenter and the polymer.

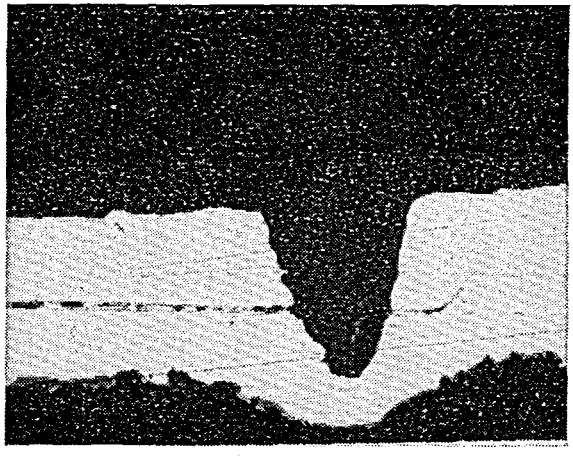

(a) P = 500 g; without plastic

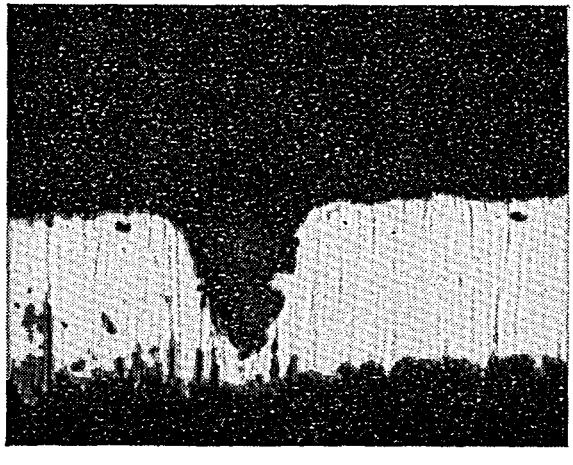

(b) P = 500 g; with plastic

A demonstration of the lifting tendency that debonds the polymer layer just outside the indented rim is shown in Figure 5. When the #5 indenter is pressed against an uncovered copper substrate (Fig. 5a and 5c) a small pileup of the copper is noted, both for $P = 200$ and 500 gram force. However, when an indentation is made on a plastic-bonded laminate (Figures 5b and 5d), the presence of the plastic tends to prevent the pileup. In order to provide this resistance, the polymer top layer must be anchored down further out,

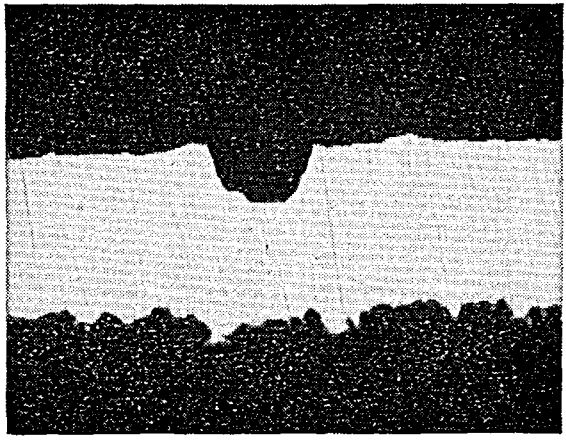

(c) P = 200 g; without plastic

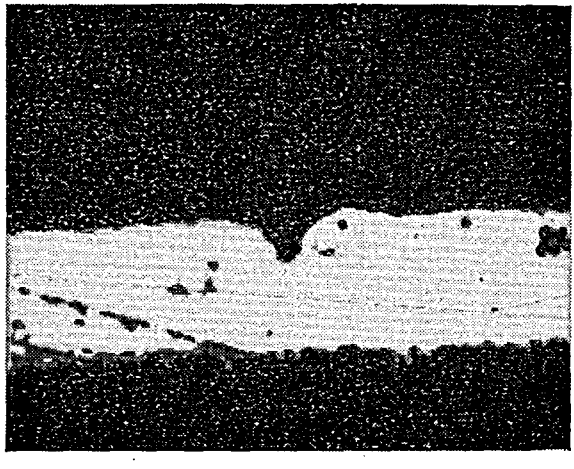

(d) P = 200 g with plastic

FIGURE 6 Indentations on copper based substrates, with #5 needle: 500× cross-sections. For needle shapes, see Figure 2.

hence the tensile bond stress. Note that the Talysurf profiles of Figures 5b and 5d were made after the plastic had been removed.

In each case, careful observation of the indented polymer top-layers indicated a puncture at the bottom of the indentation.

Observation of the plastically-deformed contact region was facilitated by cross sectioning numerous indentations. Figures 6a through 6d show a matrix of cross-section photos corresponding to the Talysurfs of Figure 5.

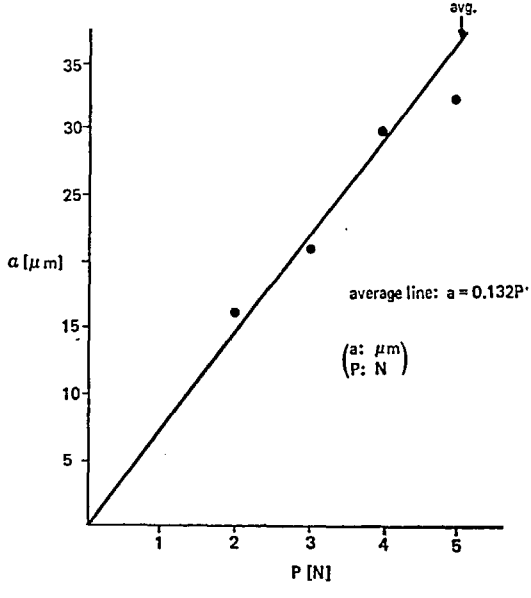

FIGURE 7 Relation between load and contact area for copper substrate (#5 needle; $h = 25$ μm).

A copper substrate of the configuration shown in Figure 1 was indented by a #5 indenter; Figures 5a and 5c were indentations on uncovered copper surfaces, while 5b and 5d were indentations through a plastic top layer of 25 μm thickness. In Figures 6b and 6d, the plastic top layer is barely visible as the assembly was enclosed in an epoxy similar to that layer, for cross sectioning.

It was apparent that the plastic deformation of the topmost copper layer closely followed the steel indenter shape, whether or not a polymer film was attached to the topmost layer.

Figure 7 shows the variation of crater radius *a vs.* the indenting force *P*, using a #5 indenter, for 25 μm plastic adhered to copper in the previous configuration (Figure 1). The data points are averaged from five sets of measurements. The obtained *a vs. P* relation is nearly linear; this is, of course,

unlike the dependency seen in a homogeneous material, where elastic deformation has $a \sim P^{\frac{1}{3}}$ and plastic deformations approach $a \sim P^{\frac{1}{2}}$.[2]

ANALYSIS

(a) Plate analysis of debonded layer

Consider the polymer top-layer perfectly conforming to the indenter contour in the central crater ($0 < r < a$), and debonding outside the crater rim up to a radius b as in Figure 8. At $r = b$, the resistance of the adhesive is sufficient

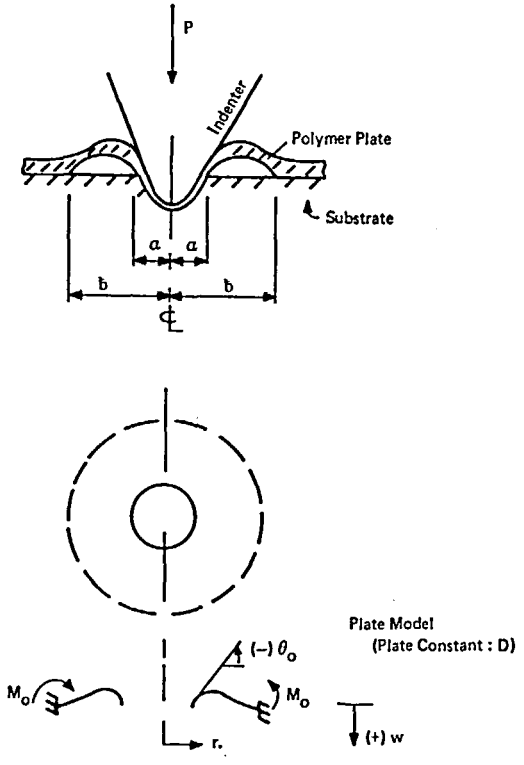

FIGURE 8 Schematic for plate action of top polymer layer.

to exert a radial moment $M_r = M_0$, securing the bond in the region $r > b$; M_0 is the "peeling moment".

Formulating this as an elastic plate problem for the plastic layer, the plate equation in polar symmetry is written[3]:

$$\frac{1}{r}\frac{d}{dr}\left[r\frac{d}{dr}\left\{\frac{1}{r}\frac{d}{dr}\left(r\frac{dw}{dr}\right)\right\}\right] = q/D \tag{1}$$

where q is the pressure distribution and D the plate flexural rigidity:

$$D = \frac{Eh^3}{12(1-\nu^2)}$$

h being the plate thickness, E the Young's modulus and ν, Poisson's ratio.

We stipulate the following boundary conditions based on the above physical reasoning:

$$r = a: \quad w = 0 \tag{2}$$

$$dw/dr = -\tan\theta_0 \tag{3}$$

$$r = b: \quad w = 0 \tag{4}$$

$$dw/dr = 0 \tag{5}$$

$$M_r = M_0 \tag{6}$$

Note that the differential displacement of the copper foundation between $r = a$ and $r = b$ has been neglected in Eqs. (2, 4) (i.e. no "sinking" is assumed).

The solution for the plate deflection, $(a \leqslant r \leqslant b)$, in the absence of loading $(q = 0)$, is well known:

$$w = c_1 r^2 + c_2 r^2 \ln r + c_3 \ln r + c_4 \tag{7}$$

Substituting for

$$M_r = -D\left(\frac{d^2w}{dr^2} + \frac{\nu}{r}\frac{dw}{dr}\right),$$

produces the following system of equations:

$$\begin{bmatrix} a^2 & a^2 \ln a & \ln a & 1 \\ 2a & 2a(\ln a + \frac{1}{2}) & 1/a & 0 \\ b^2 & b^2 \ln b & \ln b & 1 \\ 2b & 2b(\ln b + \frac{1}{2}) & 1/b & 0 \\ \hline 2(1+\nu) & 3+\nu+2(1+\nu)\ln b & \dfrac{-(1-\nu)}{b^2} & 0 \end{bmatrix} \begin{Bmatrix} C_1 \\ C_2 \\ C_3 \\ C_4 \end{Bmatrix} = \begin{Bmatrix} 0 \\ -\tan\theta_0 \\ 0 \\ 0 \\ \hline M_0/D \end{Bmatrix} \tag{8}$$

or in matrix notation:

$$\begin{bmatrix} F_1 \\ \hline F_2 \end{bmatrix} \{C\} = \begin{Bmatrix} Y_1 \\ \hline Y_2 \end{Bmatrix} \tag{9}$$

The system (8) is nonlinear as the unknowns include the coefficients $C_1, \ldots, C_4$ and the unknown debonding radius b. An alternative method of solution may fix b as a known quantity, and a subsystem of (8) is calculated for the four unknowns $C_1, \ldots, C_4$. In this case, the parameter M_0/D is calculated as a result. Figure 9 shows a family of curves for M_0 *vs.* h, with "a" varied; $b = 0.8$ mm and $\tan\theta_0 = -1$ are held constant. We see that a larger peeling moment capacity goes with increased "a" or h. It is noted that for the large

slopes achieved in the tests, θ cannot be equated with its tangent, and the analysis is, therefore, approximative as thin plate theory is used for the actual "large deflections". We shall later discuss the approximation involved.

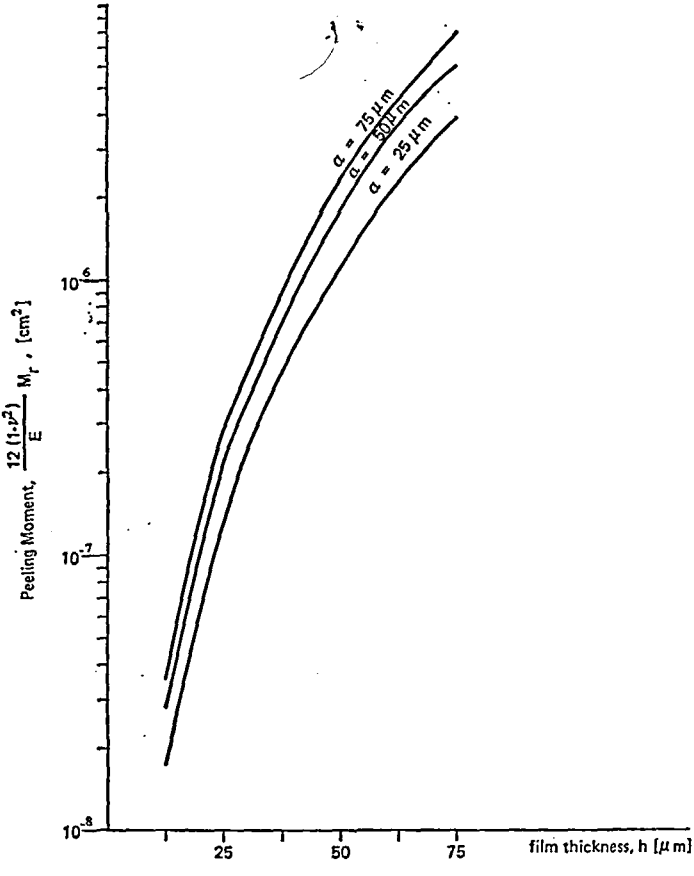

FIGURE 9 Peeling moment *vs.* plate thickness ($\tan \theta_o = -1$; $b = 0.8$ mm).

(b) Debonding-failure theory

Table I was constructed with the purpose of showing both a set of experimental force-indentation radius and corresponding force-debonding radius measurements, and the values of the M_0/D ratios at those measurements, which can be computed by the plate-analysis method of Eqs. (8) or (9). The same configuration of top- and sub-layer, indenter and materials was used in Table I as seen earlier in Figures 5 and 6.

TABLE I

Indentation series for top polymer layer of 25 μm thickness, adhered to copper-topped sandwich (see Figure 1); indentation by #5 needle point (see Figure 2) of tip-cone half angle θ_o, with $\tan \theta_o = -2.2$

Indent force, P		Indentation radius, a	Debonding radius, b	a/P	M_o/D
N	gram	μm	μm	μm/N	cm^{-1}
1.962	200	16.51	182.9	8.42	78.26
2.943	300	21.59	228.6	7.33	64.48
3.924	400	30.48	243.8	7.76	72.80
4.905	500	33.02	261.6	6.74	68.29
				Average: 7.56	Average: 70.96
		Measurement			Calculation

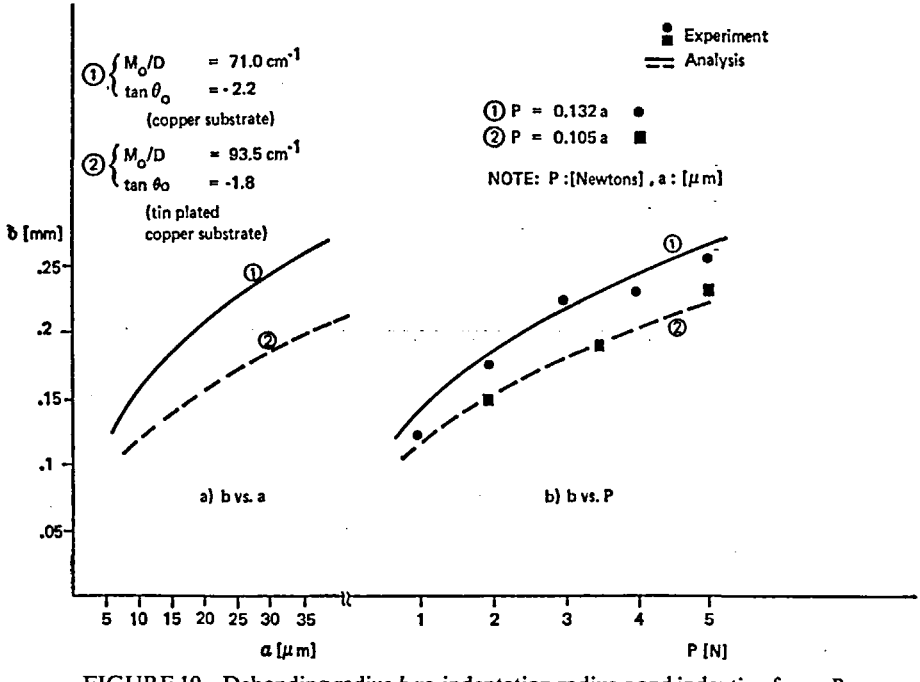

FIGURE 10 Debonding radius b *vs.* indentation radius a and indenting force P.

From Table I it is apparent that all M_0/D values associated with each case of debonding are close. For the given layer configuration (layer thickness, layer material, and bond strength to the sublayer) M_0 will now be assumed to be a characteristic "peel-moment capacity" value. If the moment capacity M_0 is known, then the desired b *vs.* P relation can be derived. Conversely, knowing the relationship of M_0/D to a more basic bond-strength parameter (involving tensile strength σ_y, etc.), then measurements of a/P can lead to the determination of whether or not the bond strength will be exceeded in a particular indentation test.

The a/P relation, which must be measured for each multilayered construction, gave the following form for the linearized test results of Table I:

$$P = 0.132\,a, \qquad (P\text{: Newtons and "}a\text{": }\mu\text{m}), \ldots \tag{10}$$

By using the fixed parameters $M_0/D = 70.96\ \text{cm}^{-1}$ and $\tan\theta_0 = -2.2$, Eqs. (8) resulted in the b *vs.* a curve shown in Figure 10a.

From this, finally the b *vs.* P curve of Figure 10b can be obtained.

DISCUSSION

We shall demonstrate the experimental-analytical procedure of obtaining a b *vs.* P relation through the example of a 25 μm thick polymer film bonded to a tin-plated copper substrate (the geometric arrangement of the layers was similar to that of Figure 1). The indenter was the #9 needle (Figure 2) with a conical tip of semiangle $\tan\theta_0 = -1.8$.

Step 1 A single load-indentation measurement was taken: at $P =$ 300 gram force, $a = 28\ \mu$m resulted. The straight-line P *vs.* a relation is then $P = 0.105a$ (in units of N and μm, respectively).

Step 2 A single debonding measurement was made: at $P = 350$ gf, $b = 192\ \mu$m was obtained.

Step 3 The value of the peel-moment capacity M_0/D is calculated as a constant parameter. From the P *vs.* a relation, at $P = 350$ g (3.44 N), $a = 3.44/0.105 = 32.8\ \mu$m. By the use of the plate Eqs. (8) with boundary conditions $a = 32.8\ \mu$m, $b = 192\ \mu$m, $\tan\theta_0 = -1.8$: $M_0/D = 93.5\ \text{cm}^{-1}$ results.

Step 4 With M_0/D known, and the P *vs.* a relation also determined, a continuous relation for P *vs.* b can be calculated, by use of the plate Eqs. (8); for every P there belongs a value of "a", and since M_0/D is constant, b is unique. Figure 10 shows the graphs together with further experimental P *vs.* b measurements for this case.

Those tests performed on the previously mentioned configurations of a

25 μm polymer layer adhered to copper and tin-plated copper indicated that the behavior of the polymer layer after debonding can be modeled for practical purposes, as an elastic plate.

The elastic plate analysis was based on thin plate theory which is an approximation in view of the large initial slopes at the rim of the indentation, $r = a$. Calculating the plate deflections $w(r)$ by Eq. (8), for the above example ($a = 32.8$ μm, $b = 192$ μm, $\tan\theta_0 = -1.8$, $M_0/D = 93.5$ cm^{-1}), the maximum displacement $w_{max} = (-)$ 28 μm was obtained at $r = 75$ μm, rather close to $r = a$. Thus displacements are of comparable magnitude as the plate thickness ($h = 25$ μm), and thin plate theory requires an adjustment[5] to account for bending moments induced by membrane forces.

In the present example, the corrected deflections come out about 50% less than those obtained by thin plate theory. This type of error is consistent throughout the range of "a" values considered, because the initial slope θ_0 is unvaried. A change to the numerical value of M_0/D results corresponding to actual debonding; however, for greater ease of calculation, the M_0/D value attained by thin plate theory may be retained, with that understanding.

The goodness of assumptions (2) and (4), neglecting the differential sinking of the foundation between $r = a$ and $r = b$, has also been checked for the above example. Normal surface displacements w_s ($r > a$) were sought for an elastic half-space indented within the circle $r \leqslant a$, by uniform load[6]:

$$w_s(r) = \frac{4(1-\nu^2)qr}{\pi E}\left[E\left(\frac{a^2}{r^2}\right) - \left(1-\frac{a^2}{r^2}\right)K\left(\frac{a^2}{r^2}\right)\right] \tag{11}$$

where E and ν are the elastic constants for the substrate, and $K(\xi)$, $E(\xi)$ are the complete elliptic integrals of the first and second kind, respectively. The fact that the half-space is plastically deformed over the loaded area does not invalidate the displacement analysis outside the loaded area, for an elastic-perfectly plastic material. Assuming a homogeneous copper substrate ($E = 111$ GPa, $\nu = 0.3$), $w_s = 0.342$ μm and 0.05 μm were obtained at $r = a$ and $r = b$, respectively. Thus, $w_s(a) - w_s(b)$ is indeed small with respect to the plate deflection.

Debonding was caused by pure interfacial separation ("adhesive failure") and as such, could be characterized by the "peeling moment" M_0. The magnitude of M_0 depended on the material of the metal substrates (e.g. copper and tin-plated copper). It also depended on the thin polymer-film thickness h in such a way, however, as to make M_0/D a constant for a given substrate material. Figure 9 shows that the thicker the film, the greater the peeling moment capacity. This study does not allow speculation as to the relationships existing when debonding depends on cohesive rather than adhesive failures of the interacting layers.

Defining the "aspect ratio" α of a bonded plate segment, as the ratio of

plate thickness to the width of the debonded segment $b-a$; i.e. $\alpha \equiv h/(b-a)$, these previous tests dealt with values of α less than $\frac{1}{6}$.

Further tests were performed on thicker ($h = 0.75$ mm) polymer top-layers with degraded bond. These layers debonded quite differently than the thinner ones, not always along the periphery of a circle but often in a semicircular shape. This situation was accentuated when the indenting force was applied with a tangential component; then the semicircular region would coincide with the indentor projection, (Figure 11a).

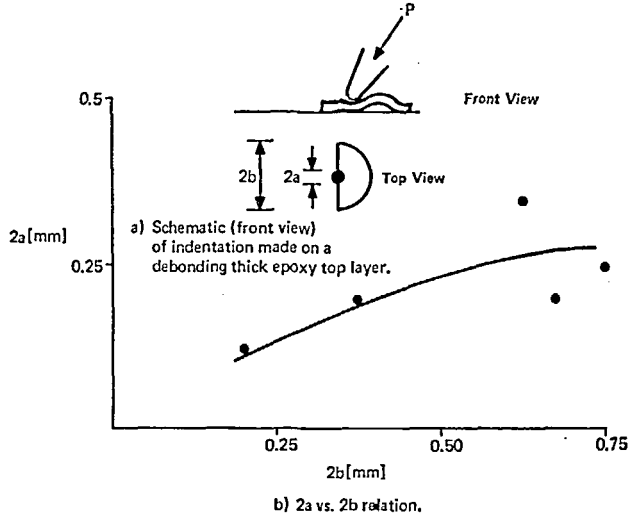

FIGURE 11 Indentation diameter *vs.* debonding diameter for 0.75 mm thick polymer layer adhered to a copper substrate.

Considering the distinguishable radius of the semicircular debonded area as b, Figure 11b was plotted as the experimental $2b$ *vs.* $2a$ relation. It is clear that the aspect ratio is now much larger ($\alpha \sim 0.5$) than it was in the previous examples of 25 μm thick layers. Therefore, the plate theory can no longer be expected to hold. Evaluating M_0/D on the basis of measured pairs of debonding cases, the resulting values were no longer found constant; they were, however, an order of magnitude higher than those found in the cases of thin (25 μm) top-layers. The debonding of the 0.75 mm thick top-layer involves "thick slab" action rather than thin plate action. The required analysis is extremely complex and is beyond the scope of this paper.

The mode of failure between polymer layer and metal substrate was investigated by Scanning Electron Microscopy (SEM). The scanning electro-micrographs (Figure 12) showing the copper and polymer sides of a debonded area (2500×) indicate the imprint of the copper surface on the polymer

surface, but the surfaces are clean. Thus debonding clearly occurred at the interface and not cohesively within the epoxy coating. The interfacial separation ("adhesive failures") shown in these pictures were promoted during preparation by the bond degradation technique.

If debonding is a function of the plate moment M_0 at the edge of the debonded area, and also of the strength of the adhesive, it is expected that a "peel-strength" theory can be found relevant in even more basic terms than the present theory. Other interesting and practical applications are expected from hard top-layer configurations which should debond in a different pattern.

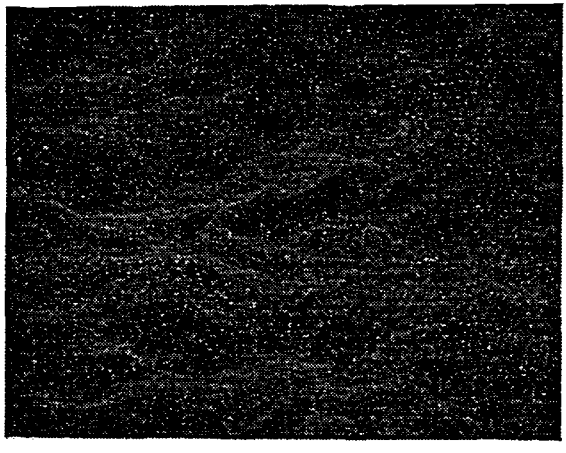

(a) Copper Side

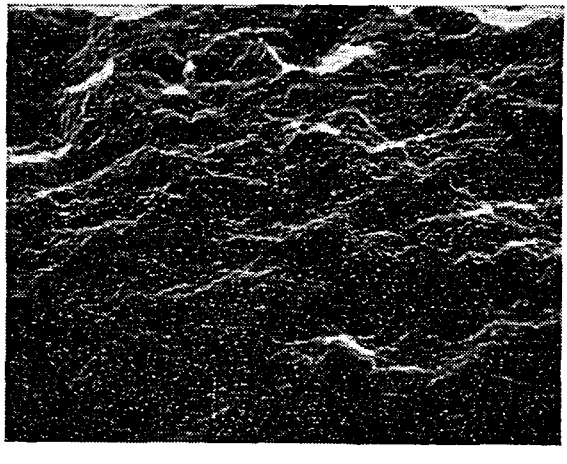

(b) Polymer Side

FIGURE 12 Scanning electromicrographs of debonded area. 2500×.

Soft top layers were influenced by plastic deformations in the contact region; hard top layers are likely to be affected by a "plate on elastic foundation" effect.

Based on the simplicity and utility of the indentation-debonding test, it can probably take its place besides such older and established bond testing methods as the peeling test and the blister test.[4] Its key advantage is that it can be performed on actual production parts.

CONCLUSIONS

The bond strength of the coating on a laminar structure subjected to mechanical indentation has been investigated. The engineering analysis requires an empirical force *vs.* displacement characteristic to be obtained from tests. Because this frequently is linear, data from a single debonding experiment have shown to be sufficient for prediction of eventual interfacial debonding of a given coating.

Acknowledgements

The authors acknowledge the help and interest of G. C. Pedroza and R. C. Ludden, and the experimental assistance of D. A. Thorne. They also thank M. A. Acitelli, E. Sacher and W. T. Chen for many lively discussions.

References

1. P. A. Engel, D. D. Roshon and D. A. Thorne, *Insulation/Circuits* 24, 35–36 (1978).
2. P. A. Engel, *Impact Wear of Materials* (Elsevier, New York, 1976).
3. S. Timoshenko and S. Woinowsky-Krieger, *Theory of Plates and Shells* 2nd ed. (McGraw-Hill, New York, 1959).
4. G. P. Anderson, S. J. Bennett and K. L. DeVries, *Analysis and Testing of Adhesive Bonds* (Academic Press, New York, 1977).
5. Reference 3, p. 400.
6. S. Timoshenko and J. N. Goodier, *Theory of Elasticity*, 3rd ed. (McGraw-Hill, New York, 1970), p. 404.

Nomenclature

a	(μm)	indentation radius	q	(N/mm²)	pressure
b	(μm)	debonding radius	r	(mm)	radial coordinate
D	(N . cm)	plate rigidity	w	(μm)	plate displacement
E	(N/mm²)	Young's modulus	w_s	(μm)	substrate displacement
h	(mm)	plate thickness	$\alpha \equiv h/(b-a)$		aspect ratio
M	(N . m/m)	plate moment	θ		slope
M_o	(N . m/m)	peeling moment	ν		Poisson's ratio
P	(N)	indenting force			